

RESEARCH PAPER

The Role of Gallium in Changing the Electrical Properties and Transfer Characteristics of Indium Arsenide-Phosphorene Heterojunction Nano-TFETs

Maryam Khorashadizadeh¹, Daryoosh Dideban^{1,2*}

¹ Institute of Nanoscience and Nanotechnology, University of Kashan, Kashan, Iran

² Department of Electrical and Computer Engineering, University of Kashan, Kashan, Iran

ARTICLE INFO

Article History:

Received 05 January 2025

Accepted 23 March 2025

Published 01 April 2025

Keywords:

DFT

Hetero-structure

Nano-structure

Tunneling Field Effect Transistor

ABSTRACT

In this work, the gallium is introduced into the structure of indium arsenide and contributed to the formation of $\text{In}_{0.53}\text{Ga}_{0.47}\text{As}$. Simulations are performed to study the behavior of indium arsenide-phosphorene heterostructure tunneling field effect transistors (TFETs). Density functional theory (DFT) in combination with non-equilibrium Green's function are utilized to reveal the electrical properties and transfer characteristics of the sample in question. Current changes in terms of applied bias voltage, indicates the multiplicity of negative differential resistance (NDRs) in the sample. At $V_{ds} = 0.5\text{V}$, the ratio of peak to valley current (I_p/I_v) is observed to be 138, 10 while at $V_{ds} = 0.1\text{V}$, I_p/I_v ratio reaches 16, 10.3. The subthreshold slope (S) at high and low drain bias is measured at 20, 17.2 mV/decade, respectively. transmission pathway shows the possible path of electrons, and in the on-state, the increase in the volume of the arrows is completely expected.

How to cite this article

Khorashadizadeh M., Dideban D. The Role of Gallium in Changing the Electrical Properties and Transfer Characteristics of Indium Arsenide-Phosphorene Heterojunction Nano-TFETs. *J Nanostruct*, 2025; 15(2):414-421. DOI: 10.22052/JNS.2025.02.003

INTRODUCTION

In order to reduce power consumption in modern very large scale integration (VLSI) systems and mobile electronic appliances, the power management in the nanoelectronic circuits is regarded as one of the most important factors [1]. Tunnel field-effect transistors (TFETs) rely on quantum-mechanical tunneling unlike conventional metal-oxide-semiconductor field-effect transistors (MOSFETs) which acts on the drift-diffusion of carriers [2]. TFETs having low leakage current and a small subthreshold swing

(S) has been widely studied as a promising ultra-low-power electronic device [3-5]. Material and device co-integration approach offers promising options for hybrid logic designs that combine the high energy efficiency of TFETs and the high performance of MOSFETs [6]. Tunnel Field-effect transistor (TFET) is regarded as the most promising candidate which can possibly replace the traditional MOSFET from current IC technology. It has gained much attention from the researchers because of its ability to achieve steep subthreshold slope, a greater immunity

* Corresponding Author Email: dideban@kashanu.ac.ir



This work is licensed under the Creative Commons Attribution 4.0 International License.

To view a copy of this license, visit <http://creativecommons.org/licenses/by/4.0/>.

towards the short-channel effects and low standby power dissipation. Although TFET promises a lot of advantages over other contenders of MOSFET, the current transport mechanism i.e., band to band tunneling (BTBT) leads to its two major roadblocks such as low ON-state current and ambipolarity[7]. The physics of two-dimensional (2D) materials and heterostructures based on such crystals has been developing extremely fast. With new 2D materials, truly 2D physics has started to appear (e.g. absence of long-range order, 2D excitons, commensurate-incommensurate transition, etc). Novel heterostructure devices are also starting to appear - tunneling transistors, resonant tunneling diodes, light emitting diodes, etc. Composed from individual 2D crystals, such devices utilize the properties of those crystals to create functionalities that are not accessible to us in other heterostructures[8]. III-V heterostructure TFETs are promising for low-power applications [9-11]. Indium gallium arsenide (InGaAs) (alternatively gallium indium arsenide, GaInAs) is a ternary alloy (chemical compound) of indium arsenide (InAs) and gallium arsenide (GaAs) [12]. Indium and gallium are (group III) elements of the periodic table while arsenic is a (group V) element. Alloys made of these chemical groups are referred to as "III-V" compounds. InGaAs has properties intermediate between those of GaAs and InAs. InGaAs is a room-temperature semiconductor with applications in electronics and photonics. The optical and mechanical properties of InGaAs can be varied by changing the ratio of InAs and GaAs, $\text{In}_{1-x}\text{Ga}_x\text{As}$.

In this work, at the first step, with introducing gallium in the structure of indium arsenide, an $\text{In}_{0.53}\text{Ga}_{0.47}\text{As}$ alloy is formed. In the second step, by creating a vertical hetero structure tunneling field effect transistor, its electronic properties are investigated. The effect of gallium on the structure of this nanotransistor was analyzed.

DEVICE STRUCTURE AND SIMULATION PROCEDURE

At the beginning, to construct a heterostructure nanotransistor, armchair phosphorene nanoribbon with lattice constants of 3.32\AA and 4.38\AA and indium arsenide with the lattice constant of 6.0583\AA were used, while gallium atoms were replaced indium atoms by 47% in the structure. A one-nanometer overlap [13] is created due to the Van der Waals interaction

between the two structures. $\text{In}_{0.53}\text{Ga}_{0.47}\text{As}$ with p-type doping acts as source and phosphorene with n-type doping is selected as the drain in this double gate nanotransistor. The channel region is comprised of both phosphorene and indium-gallium-arsenide stacks. We created a heterostructure nanotransistor, by placing the source at the left and the drain at the right side where a doping-less channel is located in the middle. The source-channel and drain-channel regions were selected without underlap. A view of the proposed heterostructure nanotransistors are shown in Fig. 1.

Both TFETs shown in Fig. 1 are comprised of a gate electrode with 3.26nm length and 0.45nm thickness, zero underlaps between gate and source/drain regions ($UL_s=UL_d=0$) and a layer of gate dielectric with half nanometer thickness. In order to study the electrical characteristics and reveal the electronic transport phenomena, two different gate voltages of 0.1V and 0.5V are applied to the gate electrode.

We perform the transport calculations within the framework of density functional theory (DFT) coupled with non-equilibrium Green's function (NEGF) method integrated in the Atomistix ToolKit (ATK) 2017.2 package [14, 15]. In optimizing structures, 'SG15' with 'Medium' basis set is employed with a density mesh cutoff of 80Ha at the electron temperature of 300K . We use the generalized gradient approximation (GGA) of Perdew-Burke-Ernzerh form (PBE) [16] for the exchange correlation functional.

The Monkhorst-Pack k-points of $1\times 1\times 50$ is used in the irreducible Brillouin zone (IBZ), which is dense enough for convergence. The calculations are iterated self-consistently until the energy is converged to 10^{-4}Ha . After forming the heterostructure and to investigate the transfer characteristics, calculation is performed with Extended-Huckel basis for phosphorus, indium, arsenic and hydrogen atoms with a mesh cutoff of 75Ha and k-point sampling of $13\times 1\times 108$.

We calculate the transmission coefficient at k_x point $T(E, k_x)$ (Eq. 1), Where $G^{r/a}$ and $\Gamma_{s/d}$ are the retarded/advanced Green's function and the source/drain level broadening, respectively. The transmission coefficient $T(E)$ an average of $T(E, k_x)$ over $57 k_x$ -points in IBZ. The current at a given V_{ds} and V_g is then calculated from the transmission coefficient $T(E)$, which is regarded as the Landauer-Büttiker formula [17] (Eq. 2):

$$T(E, k_x) = \text{Tr}[G^r(E, k_x) \cdot \Gamma_s(E, k_x) \cdot G^a(E, k_x) \cdot \Gamma_d(E, k_x)] \quad (1)$$

$$I(V_{ds}, V_g) = \frac{2e}{h} \int_{-\infty}^{+\infty} \{T(E, V_{ds}, V_g)[f_s(E - \mu_s) - f_d(E - \mu_d)]\} dE \quad (2)$$

Where f_s/f_d and μ_s/μ_d are the Fermi-Dirac distribution functions and electrochemical potentials of the source/drain, respectively.

RESULTS AND DISCUSSIONS

Fig. 2 illustrates the transfer characteristics of proposed heterogeneous TFET at low and high

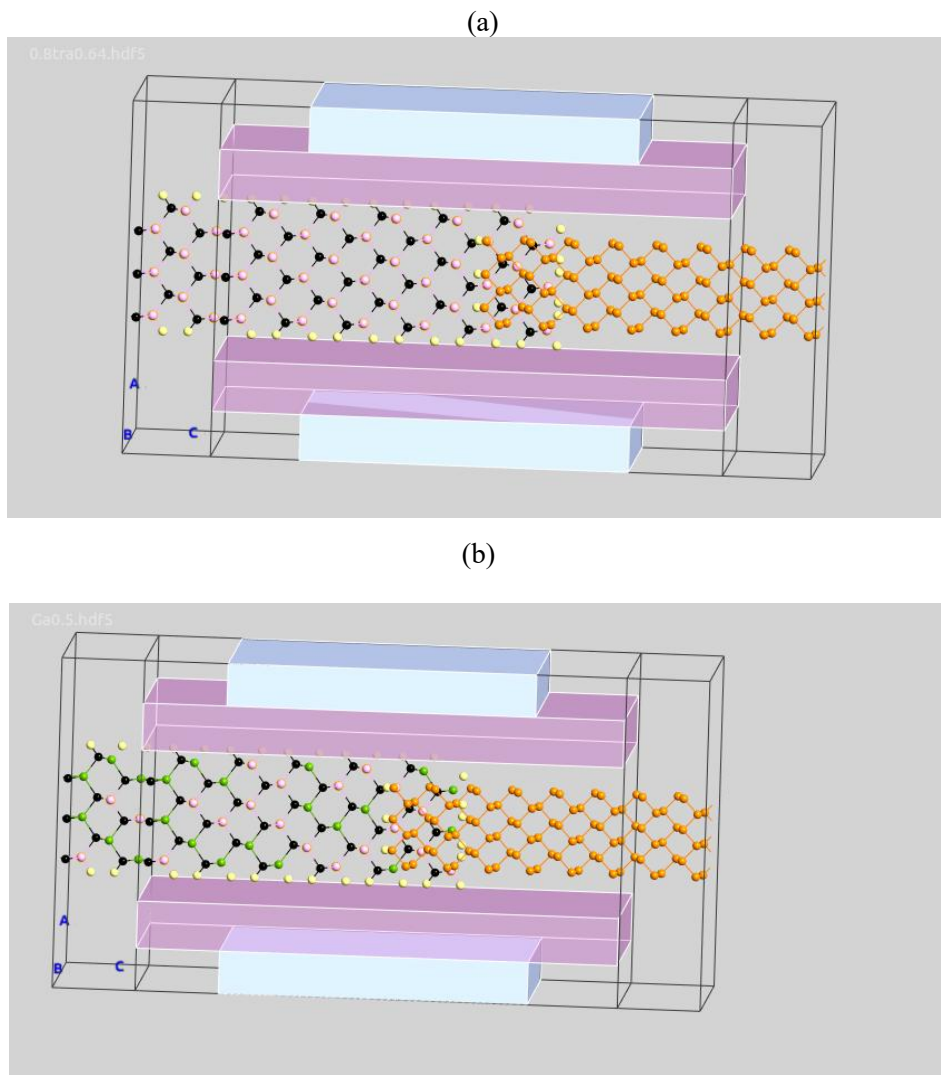


Fig. 1. Schematic view of the sub-5 nm heterostructure nano-TFET: (a) InAs-P channel, (b) $\text{In}_{0.53}\text{Ga}_{0.47}\text{As}$ -P channel. Different colors represent various atoms in the structure: H(yellow), P(brown), In(black), As(pink) and Ga(green). Please note that the channel is rotated 90° in this schematic to better represent different atoms along the device.

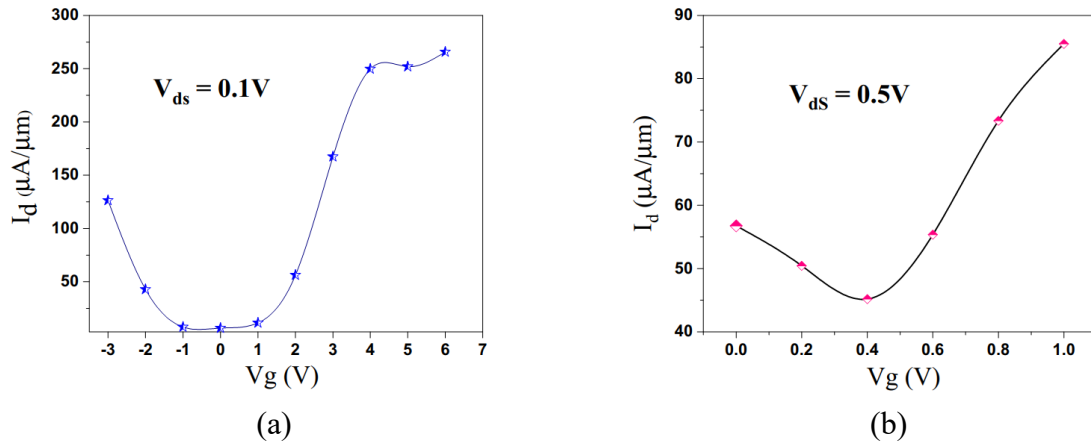


Fig. 2. Transfer characteristics for the proposed heterojunction TFET with overlap of approximately 1nm in (a) low and (b) high drain bias, respectively.

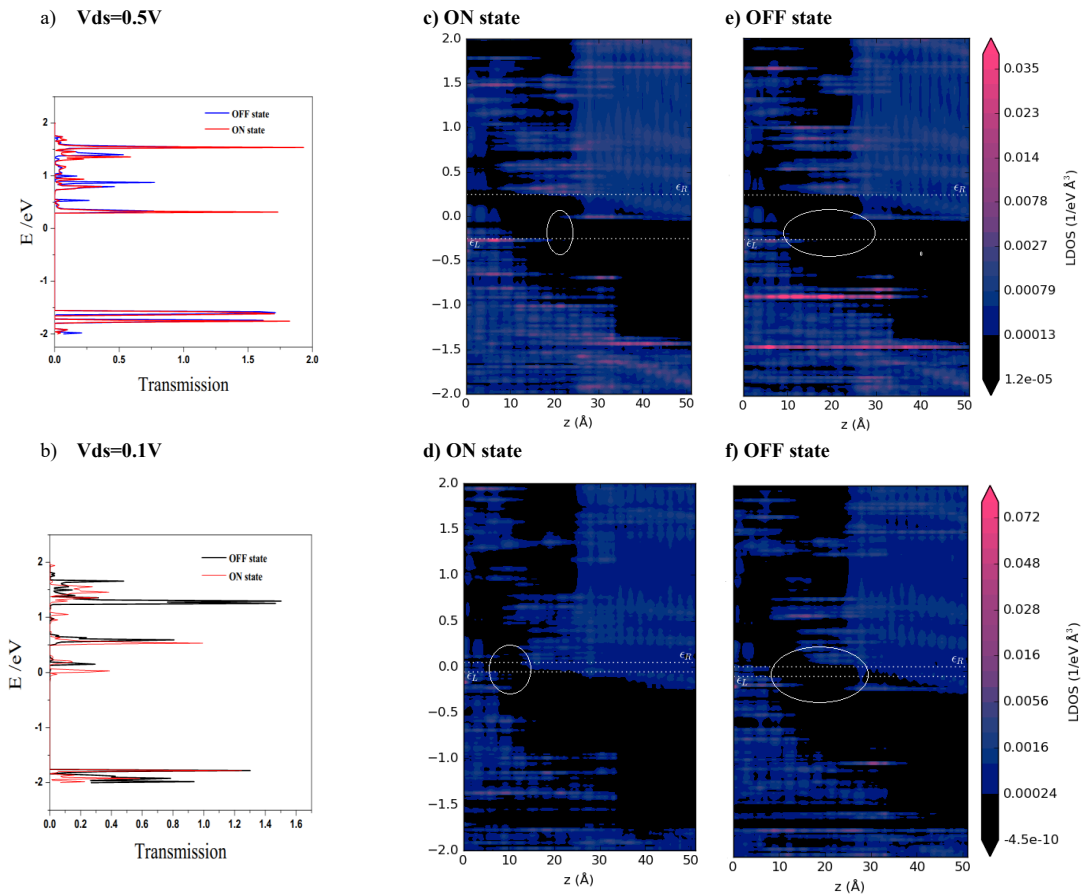


Fig. 3. (a, b) Transmission spectra, (c, e) Partial local density of states (PLDOS) under high performance for on/off-states, (d, f) PLDOS under low performance for on/off-states. Please note that all of the graphs belong to the proposed heterojunction TFET with $L_g=3.26nm$

drain bias corresponding to $V_{ds} = 0.1V$, $V_{ds} = 0.5V$, respectively. From Fig. 2(a) it can be seen that by changing the gate voltage in the range of -3 to 6 volts, the ambipolar phenomenon is occurred and the Dirac point is located at the zero gate voltage. The maximum current occurs at $V_g=6V$, with the quantity of $256 \mu A/\mu m$. At the zero gate voltage the lowest current intensity happens.

In the transfer characteristics shown in Fig. 2(b), which belongs to high-drain bias of 0.5V (high performance), the gate voltage range varies from zero to 1 volt. Although the current intensity is less than the low drain bias mode, there is still the evidence of a Dirac point as well as ambipolar conduction in this case. The maximum current in this case is $85 \mu A/\mu m$ and occurs at $V_g=1V$.

The value of the subthreshold slope is measured as 20mV/decade at high performance and 17mV/decade at low performance mode. It is improved in comparison with other similar works, either heterojunction TFET made with $WSe_2/SnSe_2$ [18] or homojunction TFET utilized $SnSe$ [19]. Also the works done on other materials [20-23] and research on $InGaAs/InAs/InGaAs$ [24] have been conducted in recent years.

In order to further analyze the conduction mechanism, the corresponding PLDOS (Partial Local Density of States) and transmission spectra were calculated. In Fig. 3(a, b) transmission spectrum for high and low performance is plotted. In Fig. (3a), we draw the value of the transmission coefficient for the ON and OFF states of the proposed nano-TFET. Higher peaks for the transmission intensity

in the on- state are observed. Peaks of varying intensity in half of the bias window can be seen which is clearly consistent with PLDOS spectrum shown in Fig. 3(c, e). It seems that the voltage applied to the side gates did not apply such a strong electric field that the whole bias window can be located outside the energy gap [25]. Fig. (3b) shows transmission coefficient for $V_{ds}=0.1V$. In this case, we see peaks in the bias window. The intensity of the peaks is significant in the on-state compared to the off state.

NDR (negative differential resistance) is a nonlinear carrier transport phenomenon whereby the electric current decreases with increasing of the bias voltage [26]. The NDR effect can also be understood by comparing the transmission spectra when the current reaches a peak and valley [27]. The effect of negative differential resistance for indium-gallium-arsenide sample is investigated in high and low performance in the bias voltage range of 0-1.4 V and 0-2 V, respectively.

As shown in Fig. 4, we see multiple peak and valley points in the output characteristics. It is worth noting that in the absence of gallium in the structure, NDR phenomenon in low performance is not observed. However, with the presence of gallium in the $InGaAs/P$ heterojunction nano-TFET, multiple NDR effects is manifested in both low and high performance conditions. At $V_{gs} = 0.5V$, three peaks can be seen at $82.8, 125$ and $485.5 \mu A/\mu m$. Measured peak to valley ratio current (I_p/I_v) is 138 and 10, respectively. For low performance mode ($V_{gs} = 0.1V$), the presence of two peaks can be seen

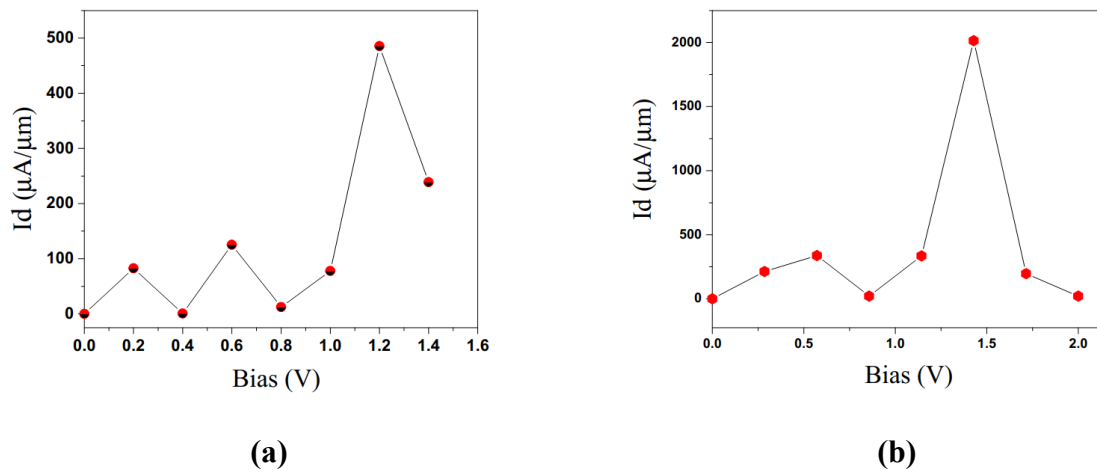


Fig. 4. The I-V_{bias} output curves for proposed heterostructure nano-TFET in (a): $V_{gs} = 0.5V$ (b) $V_{gs} = 0.1V$.

in 337 and 2014 $\mu\text{A}/\mu\text{m}$. Measured I_p/I_v in this case is either 16 or 10.

The transmission eigenstate is a complex 3-D wave function and is illustrated by an isosurface with isovalue given by the magnitude of the eigenstate. The color maps represent the phase of the eigenstate [28]. For a visual understanding of the electronic transmission mechanism, the transmission eigenstates in the on-state and off-state are given in Fig. 5. The wave functions were replaced on the source side. When the transistor becomes on, they extend to the center and drain side. The difference between on/off states is clearly consistent with current diagrams and

transmission spectra.

When the system is divided into two parts A and B, the transmission pathway of the electrons through the A and B boundaries is the sum of total transmission coefficients [29,30]. The transmission pathway can split the transmission coefficients into the contribution of local bond T_{ij} and it can be both positive and negative.

$$T(E) = \sum_{i \in A, j \in B} T_{ij}(E) \quad (3)$$

Positive T_{ij} indicates the electrons forward

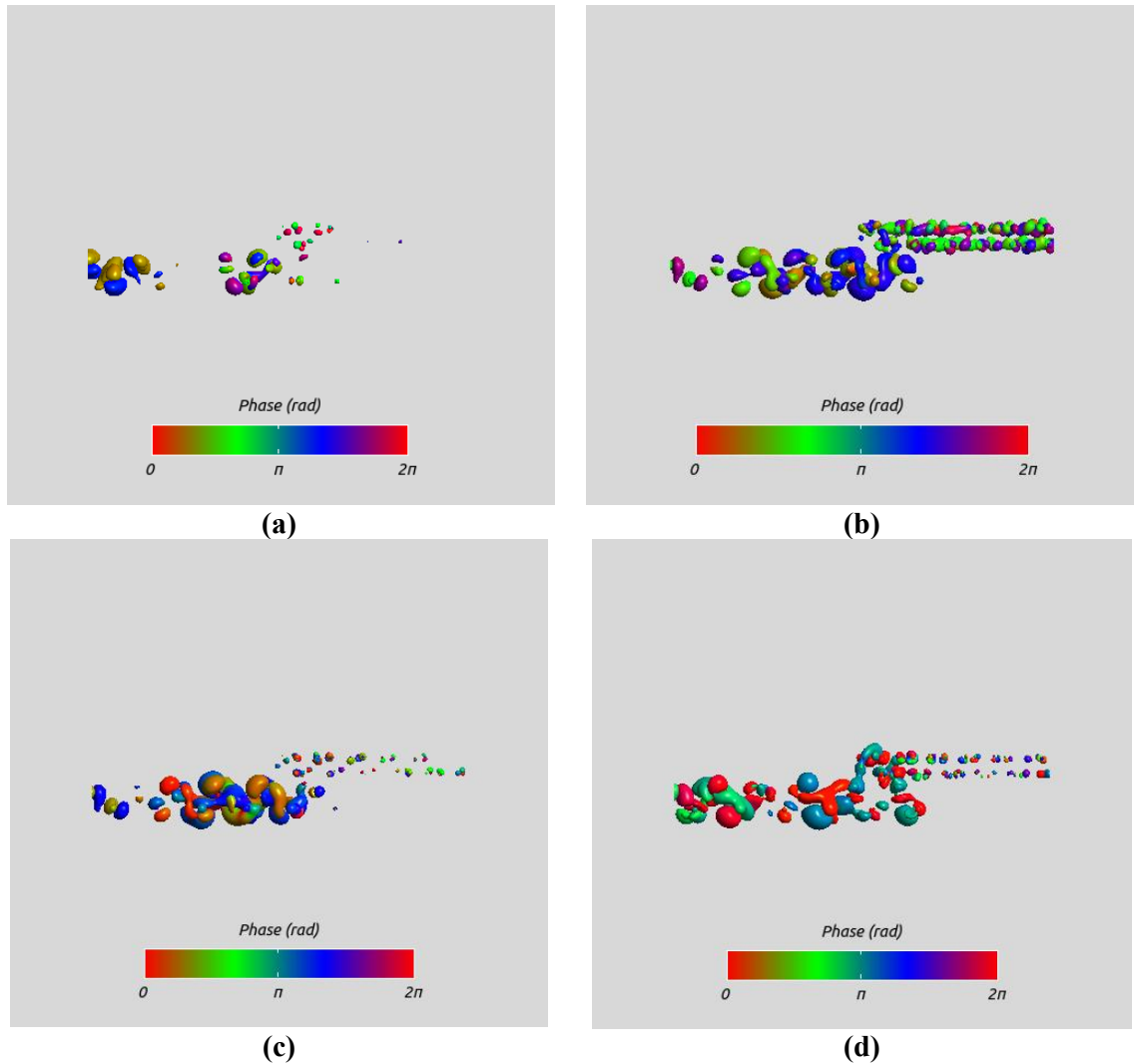


Fig. 5. Transmission eigenstates in proposed nano-TFET for: (a, b) off/on state of low performance in $V_{ds} = 0.1\text{V}$, (c, d) off/on state of high performance in $V_{ds} = 0.5\text{V}$. The isovalue is 0.1 a.u.

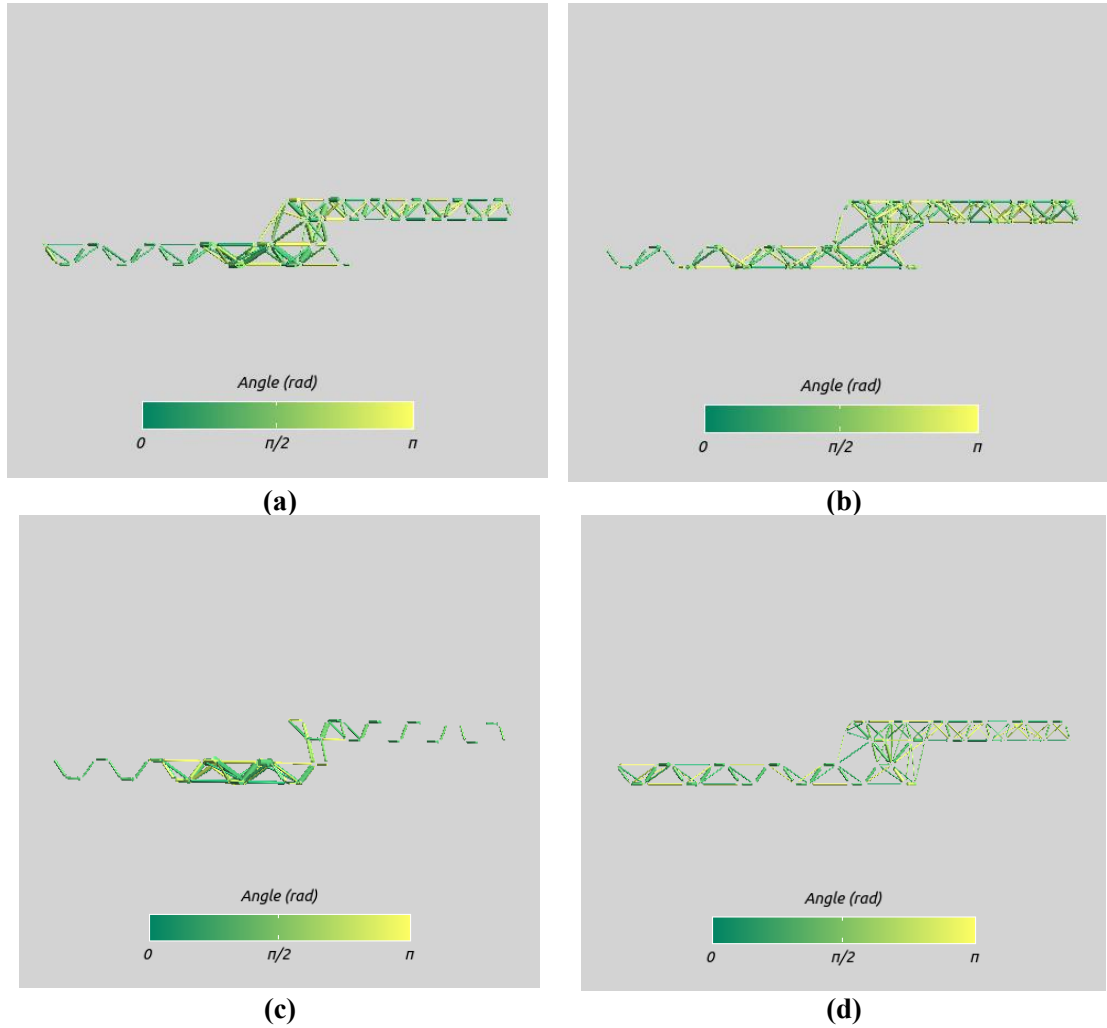


Fig. 6. Transmission pathway of electrons in the proposed nano-TFET: (a, b) on/off state for low performance i.e. $V_{ds} = 0.1V$, (c, d) on/off state for high performance i.e. $V_{ds} = 0.5V$

scattered along the bond and it is visualized as the arrow from i to j . On the contrary, negative T_{ij} indicates the electrons back-scattered along the bond and it is visualized as the arrow from j to i . Therefore, the arrows of the transmission pathway indicate the direction of the electrons transmission [30]. The transmission pathway is shown in Fig. 6. The arrows indicate the possible electron transfer path. Figs. 6(a-c) show the off-state while Figs. 6(b-d) show the on-state in nano-TFET under study. The volume of the arrows is significant in the on-state at the overlap area and on the drain side.

CONCLUSION

An $\text{In}_{0.53}\text{Ga}_{0.47}\text{As}$ /Phosphorene heterojunction

TFTE as nano-device has been proposed and studied. Numerous device analysis were performed at high and low performance. It was revealed that this transistor can be further studied due to its NDR multiplicity as a very fast switching device at high and low voltages. Calculation of the subthreshold slope at high and low performance of 20 and 17.2 mV/decade was obtained, which has been improved due to the presence of gallium in the structure.

For a visual understanding of the electronic transmission mechanism, we used transmission eigenstate and transmission pathway. With the presence of gallium, we have witnessed the NDR phenomenon with current values of 82.8, 125 and

485.5 μ A/ μ m with gate voltage of 0.5V while the current values equal to 337 and 2014 μ A/ μ m were observed with the gate voltage of 0.1V.

ACKNOWLEDGEMENTS

This research was supported by University of Kashan under supervision of Dr. Daryoosh Dideban. Authors are thankful to the support received for this work from Microelectronics Lab (meLab) at the University of Glasgow, United Kingdom.

CONFLICT OF INTEREST

The authors declare that there is no conflict of interests regarding the publication of this manuscript.

REFERENCES

- Natarajan V, Nagarajan AK, Pandian N, Savithri VG. Low Power Design Methodology. Very-Large-Scale Integration: InTech; 2018.
- Convertino C, Zota CB, Schmid H, Caimi D, Czornomaz L, Ionescu AM, et al. A hybrid III–V tunnel FET and MOSFET technology platform integrated on silicon. *Nature Electronics*. 2021;4(2):162-170.
- Kim KR, Yoon YJ, Cho S, Seo JH, Lee J-H, Bae J-H, et al. InGaAs/InP heterojunction-channel tunneling field-effect transistor for ultra-low operating and standby power application below supply voltage of 0.5 V. *Current Applied Physics*. 2013;13(9):2051-2054.
- Babu KMC, Goel E. Evolution of Tunnel Field Effect Transistor for Low Power and High Speed Applications: A Review. *Silicon*. 2022;14(17):11051-11060.
- Chander S, Sinha SK, Chaudhary R. Comprehensive review on electrical noise analysis of TFET structures. *Superlattices Microstruct*. 2022;161:107101.
- Lanuzza M, Strangio S, Crupi F, Palestri P, Esseni D. Mixed Tunnel-FET/MOSFET Level Shifters: A New Proposal to Extend the Tunnel-FET Application Domain. *IEEE Trans Electron Devices*. 2015;62(12):3973-3979.
- Karthik KRN, Pandey CK. A Review of Tunnel Field-Effect Transistors for Improved ON-State Behaviour. *Silicon*. 2022;15(1):1-23.
- Novoselov KS, Mishchenko A, Carvalho A, Castro Neto AH. 2D materials and van der Waals heterostructures. *Science*. 2016;353(6298).
- Convertino C, Zota CB, Schmid H, Ionescu AM, Moselund KE. III–V heterostructure tunnel field-effect transistor. *J Phys: Condens Matter*. 2018;30(26):264005.
- Lind E, Memisevic E, Dey AW, Wernersson L-E. III-V Heterostructure Nanowire Tunnel FETs. *IEEE Journal of the Electron Devices Society*. 2015;3(3):96-102.
- Zhu Y, Hudait MK. Low-power tunnel field effect transistors using mixed As and Sb based heterostructures. *Nanotechnology Reviews*. 2013;2(6):637-678.
- Pearsall T. Ga_{0.47}In_{0.53}As: A ternary semiconductor for photodetector applications. *IEEE J Quantum Electron*. 1980;16(7):709-720.
- Li H, Lu J. Sub-10 nm vertical tunneling transistors based on layered black phosphorene homojunction. *Appl Surf Sci*. 2019;465:895-901.
- Michelsen MM, Mygind ND, Frestad D, Prescott E. Women with Stable Angina Pectoris and No Obstructive Coronary Artery Disease: Closer to a Diagnosis. *European cardiology*. 2017;12(1):14-19.
- Brandbyge M, Mozos J-L, Ordejón P, Taylor J, Stokbro K. Density-functional method for nonequilibrium electron transport. *Physical Review B*. 2002;65(16).
- Perdew JP, Burke K, Ernzerhof M. Generalized Gradient Approximation Made Simple. *Phys Rev Lett*. 1996;77(18):3865-3868.
- Barker JR, Watling JR. A semi-empirical technique for simulating mesoscopic quantum transport in warped band structures. *Microelectron Eng*. 1999;47(1-4):369-371.
- Oliva N, Backman J, Capua L, Cavalieri M, Luisier M, Ionescu AM. WSe₂/SnSe₂ vdW heterojunction Tunnel FET with subthermionic characteristic and MOSFET co-integrated on same WSe₂ flake. *npj 2D Materials and Applications*. 2020;4(1).
- Li H, Liang J, Xu P, Luo J, Liu F. Vertically stacked SnSe homojunctions and negative capacitance for fast low-power tunneling transistors. *RSC advances*. 2020;10(35):20801-20808.
- Bayani AH, Dideban D, Voves J, Moezi N. Investigation of sub-10nm cylindrical surrounding gate germanium nanowire field effect transistor with different cross-section areas. *Superlattices Microstruct*. 2017;105:110-116.
- Bayani AH, Dideban D, Moezi N. Impact of uniaxial compressive strain on physical and electronic parameters of a 10 nm germanene nanoribbon field effect transistor. *Superlattices Microstruct*. 2016;100:198-208.
- Bayani AH, Dideban D, Akbarzadeh M, Moezi N. Benchmarking Performance of a Gate-All-Around Germanium Nanotube Field Effect Transistor (GAA-GeNTFET) against GAA-CNTFET. *ECS Journal of Solid State Science and Technology*. 2017;6(4):M24-M28.
- Samipour A, Dideban D, Heidari H. First Principles Study of the Ambipolarity in a Germanene Nanoribbon Tunneling Field Effect Transistor. *ECS Journal of Solid State Science and Technology*. 2019;8(12):M111-M117.
- Baskaran S, Saravana Kumar R, Saminathan V, Poornachandran R, Mohan Kumar N, Janakiraman V. Impact of High-K and Gate-to-Drain Spacing in InGaAs/InAs/InGaAs-based DG-MOS-HEMT for Low-leakage and High-frequency Applications. *IETE Journal of Research*. 2021;69(3):1222-1232.
- Zhang W, Ragab T, Basaran C. Electrostatic Doping-Based All GNR Tunnel FET: An Energy-Efficient Design for Power Electronics. *IEEE Trans Electron Devices*. 2019;66(4):1971-1978.
- Kobashi K, Hayakawa R, Chikyow T, Wakayama Y. Negative Differential Resistance Transistor with Organic p-n Heterojunction. *Advanced Electronic Materials*. 2017;3(8).
- Feng S, Zhang Q, Yang J, Lei M, Quhe R. Tunneling field effect transistors based on in-plane and vertical layered phosphorus heterostructures *. *Chinese Physics B*. 2017;26(9):097401.
- Xie H-Q, Li J-Y, Liu G, Cai X-Y, Fan Z-Q. High-Performance Schottky-Barrier Field-Effect Transistors Based on Monolayer SiC Contacting Different Metals. *IEEE Trans Electron Devices*. 2019;66(12):5111-5116.
- Solomon GC, Herrmann C, Hansen T, Mujica V, Ratner MA. Exploring local currents in molecular junctions. *Nat Chem*. 2010;2(3):223-228.
- Rui C, Shao C, Liu J, Chen A, Zhu K, Shao Q. Transport properties of B/P doped graphene nanoribbon field-effect transistor. *Mater Sci Semicond Process*. 2021;130:105826.